expression, probably because of its restricted nature. Brown, W. *Ark. Kemi* **1961**, *18*, 227.
(11) It should be pointed out that eq 15-17 cannot be applied to the special case of $k_i = k_x$, since they contain reciprocals of $k_x - k_i$. The appropriate equation for this particular and, probably, rare case is $Y_{ni} = (B^n k_i^n/n!) \exp(-Bk_i)$.
(12) Wirick, M. G. *J. Polym. Sci., Part A-1* **1968**, *6*, 1705.
(13) Klop, W.; Kooiman, P. *Biochim. Biophys. Acta* **1965**, *99*, 102 and references therein.
(14) Equation 29 describes the number of chain breaks as measured conveniently by the change in the degree of polymerization.[12,13] It can be shown by computation that as S_0 increases C will increase to a maximum of 0.144 at $S_0 \simeq 0.6$. However, C will decrease with further increase in S_0, reaching zero at $S_0 = 1$. Thus, the applicability of this treatment is limited to materials with $S_0 < 0.6$. HEC products of interest have fairly high degrees of substitution,[5] and the mole fraction of unsubstituted glucosyl residues is usually $S_0 < 0.3$.[6,12]

Model Reaction Pathways in Kraft Lignin Pyrolysis

Francis P. Petrocelli and Michael T. Klein*

Department of Chemical Engineering, University of Delaware, Newark, Delaware 19711.
Received April 12, 1983

ABSTRACT: Kraft lignin pyrolysis was analyzed in terms of the experimental thermolyses of 1,2-diphenylethane, *cis*- and *trans*-stilbene, diphenylmethane, and triphenylethylene, all compounds mimicking prevalent Kraft lignin structural moieties. The experiments revealed five first-order diphenylethane pyrolysis pathways, the most important of which led to formation of toluene. Degradative pyrolysis of either stilbene isomer was equivalent to decomposition of a near-equilibrium mixture in which trans was prevalent. Diphenylmethane pyrolysis yielded benzene, toluene, and fluorene, and triphenylethylene pyrolyzed to these three and also diphenylmethane, diphenylethane, stilbene, and phenanthrene. All Arrhenius parameters of the pyrolysis pathways were determined. The present results are used in analysis of the thermal reactions of Kraft lignin. Of note, reaction pathways for the formation of methyl-substituted phenolics and hydroxyl-substituted fused-ring aromatics are developed.

Introduction

Conversion of macromolecular resources to lower molecular weight chemicals will be enhanced through elucidation of the process-controlling reaction pathways, kinetics, and mechanisms. Lignin pyrolysis to gas, liquid, tar, and char product fractions, for example, yields both useful and undesirable components, and strategies for selective production of useful products remain unclear on account of the complexity of both the lignin structure and its pyrolysis product spectra. These complexities motivate the use of simple model compounds whose chemical structures mimic structural residues found in the macromolecule. The relatively simple product spectra obtained from model compound pyrolyses allow inference of a macromolecule's operative pyrolysis pathways, kinetics, and, in favorable cases, mechanisms. The present analysis of Kraft lignin pyrolysis, then, is as discerned through the experimental pyrolyses of the model compounds 1,2-diphenylethane (DPE), *cis*- and *trans*-stilbene, diphenylmethane (DPM), and triphenylethylene (TPE).

Structural analyses (Freudenberg, 1968; Glasser, 1981) show native lignin to be a copolymer of single-ring phenolic units that can be characterized by the bonds that connect them and also by the substituents each ring possesses (Klein and Virk, 1981). For the present analysis the influence of Kraft pulping on the types and proportions of substituents and interunit links that a Kraft lignin comprises was inferred from the structural scenario presented by Marton (1971).

Comparison of native and Kraft lignin structural information shows that the α- and β-aryl alkyl ether linkages so prevalent in native lignins are scarce in Kraft lignins and are replaced, in large part, by diphenylethane, diphenylmethane, stilbene, and triphenylethylene linkages; other Kraft lignin linkages are akin to biphenyl, diphenyl ether, and phenethyl phenyl ether (PPE) molecules. Since only one PPE linkage appears in the Marton structure and biphenyl and diphenyl ether linkages are thermally stable (Klein, 1981), the present analysis was formulated in terms of the pyrolyses of the hydrocarbons diphenylethane, stilbene, diphenylmethane, and triphenylethylene. By extending similar analyses of native lignins and the oxygen-containing interunit linkages contained therein (Klein and Virk, 1983) to include hydrocarbon reactions, this analysis should therefore reveal the essential differences between native and Kraft lignin pyrolysis.

Previous Kraft lignin pyrolyses provided a framework for the analysis. Iatridis and Gavalas (1979) reported the yields of permanent gases, methanol, acetone, and five single-ring phenolics as a function of pyrolysis temperature and time. Connors et al. (1980) found phenols, guaiacols, catechols, char, methane, and carbon dioxide from pyrolysis in tetralin. Chan and Krieger (1981) detailed the yields and components of gas, aqueous distillate, phenolic, and carbonaceous residue product fractions obtained from microwave pyrolysis, and their identification of fused-ring fluorene, anthracene, and naphthalene products from the single-ring lignin substrate is noteworthy. Graef et al. (1979) found the fused-ring naphthalene, anthracene, and acenaphthene products from microwave-induced plasma pyrolysis of lignin. These pyrolyses of actual lignins have provided useful product spectra information but have yet to reveal the operative reaction pathways and intrinsic chemical kinetics involved. This motivated the present approach.

Previous pyrolyses of the model compounds are also informative. Pyrolysis of diphenylethane (DPE) in hydrogen-donor solvent occurs with solvent-independent first-order kinetics and yields a rather simple solvent-dependent product spectrum in which toluene is the major component (Brower, 1977; Collins et al., 1977; Cronauer et al., 1978; Panvelker et al., 1982; Benjamin et al., 1978; Kamiya et al., 1979). Arrhenius parameters are similar for liquid- and gas-phase pyrolyses (Sato et al., 1978), although product spectra from the latter are more like those from thermolysis in the absence of donor solvent, where, in

0024-9297/84/2217-0161$01.50/0

Table I
Experimental Conditions for Kraft Lignin Model Compound Pyrolyses

substrate	init press, atm	pyrolysis temp, °C	holding time, s	reaction phase	init concn, mol/l	inert/substrate ratio, wt/wt
1,2-diphenylethane (DPE)	13.5	400	900-10800	vapor	0.1	1.0
	11.5-90.4	450	300-3600	vapor, mixed	0.04-1.37	0.1-1.0
	16.5	550	90-600	vapor	0.1	1.0
cis-stilbene	1.9	250	600-64800	liquid	2.0	1.0
	2.1	300	450-7200	liquid	0.2-1.9	1.0-16.0
	2.3	350	150-3600	liquid	2.0	1.0
	12.1	400	900-10800	mixed		1.0
	14.6	450	120-9000	vapor	0.1	1.0
	16.7	550	90-600	vapor	0.1	1.0
trans-stilbene	1.9	250	10800-64800	liquid	2.0	1.0
	2.1	300	300-7200	liquid	2.0	1.0
	2.3	350	150-3600	liquid	2.0	1.0
	12.1	400	900-12600	mixed		1.0
	14.6	450	120-9000	vapor	0.04-1.11	0.1-1.0
	16.7	550	90-900	vapor	0.1	1.0
diphenylmethane (DPM)	19.8-61.0	550	900-7200	vapor	0.14-0.75	0.2-1.0
	18.0	600	120-1200	vapor	0.1	1.0
triphenylethylene (TPE)	8.5	400	600-10800	liquid	1.1	1.0
	14.4-48.2	550	60-900	vapor	0.06-0.56	0.1-1.0

addition to toluene, formation of benzene, ethylbenzene, styrene, stilbenes, phenanthrene, 1,1-DPE, 1,2,3,4-tetraphenylbutane, biphenyl, diphenylmethane, fluorene, 1,2,3-triphenylpropane, and light gases like hydrogen and methane occurs (Vernon, 1980; Miller and Stein, 1979; Benjamin, 1978; Horrex and Miles, 1951; Madison and Roberts, 1958; Sweeting and Wilshire, 1962; Poutsma, 1980). Most mechanistic interpretations of DPE pyrolysis involve free-radical steps (Horrex and Miles, 1951; Sweeting and Wilshire, 1962; Vernon, 1980; Poutsma, 1980; Miller and Stein, 1979), although Virk (1979) has explained experimental product spectra in terms of a pericyclic mechanism in accord with the Woodward–Hoffmann (1970) conservation of orbital symmetry rules.

Stilbene pyrolysis reactions include isomerization at 320–341 °C (Kistiakowsky and Smith, 1934) and decomposition to toluene, DPE, stilbene, and a black polymer at 400 °C (Benjamin, 1978). Diphenylmethane (DPM) was essentially unconverted after pyrolysis in tetralin at 400 °C and 18 h (Benjamin et al., 1978), and higher temperature pyrolyses (Madison and Roberts, 1958; Sweeting and Wilshire, 1962) produced gas (mostly H_2) and heavier products, including benzene, toluene, fluorene, triphenylmethane, tetraphenylethylene, tetraphenylethane, and phenylfluorene. Finally, triphenylethylene (TPE) and 1,1,2-triphenylethane pyrolyses in tetralin yielded diphenylmethane and toluene (Collins et al., 1977; Benjamin et al., 1978).

In summary, although previous DPE pyrolysis studies provide much useful information, far less attention has been devoted to stilbene, triphenylethylene, and diphenylmethane pyrolyses. Further, no use of any of these results has been made in analysis of Kraft lignin pyrolysis. This motivated the present work.

In summary of what follows, the first of the remaining sections concerns experimental and analytical methods. We then present experimental results, which are followed by a discussion that compares the highlights of this and previous work and also the implication of the present results to actual Kraft lignin pyrolyses. Finally, important conclusions are listed.

Experimental Section

Table I lists the pyrolysis substrates and the experimental conditions of pyrolysis temperature, holding time, reaction phase, initial reactant concentration, and ratio of added inert to reactant.

The substrates were all commercially available and used as received. Pyrolysis reactors were $^1/_4$-in. 316-stainless steel "tubing bombs" comprising one Swagelok port connector and two Swagelok caps and had 0.6-cm^3 internal volume.

Bubble and dew point calculations (at the reaction temperature) allowed execution of both vapor- and liquid-phase pyrolyses. In both cases, a representative experimental procedure was as follows. First, substrate (~10 mg) and biphenyl (~10 mg) were loaded into room-temperature tubing bombs. Stable at temperatures less than 550 °C (Klein, 1981; Vernon, 1980), biphenyl could be used both as an internal standard for later chromatographic determination of product yields and also as a diluent for the liquid-phase pyrolyses; for the pyrolyses above 550 °C, the biphenyl was added as an external standard after completion of the reaction. After flushing with volumes of nitrogen, which served as an internal standard for later gas analyses, sealed reactors were immersed in a fluidized sand bath held constant at the desired pyrolysis temperature and, after reaction, inserted into an ice–water bath.

Quenched reactors were dried and their contents analyzed for both gas- and condensed-phase products. Gas yields never exceeded 0.8 wt % of the original substrate and were therefore neglected in all cases. Condensed-phase products were collected in approximately 0.3–0.5 cm^3 of methylene chloride and analyzed on an HP 5880 gas chromatograph equipped with a flame ionization detector. Products were separated on a 6-ft-long $^1/_8$-in. packed column containing either 3% or 6% OV-17 stationary phase and identified by coinjection of reference standards, including benzene, toluene, styrene, ethylbenzene, DPM, *cis*- and *trans*-stilbene, fluorene, phenanthrene, TPE, and anthracene. Analysis of standard reference blends enabled measurement of quantitative product response factors. These in turn permitted determination of material balance closure, here defined as the ratio of the product spectrum weight to the original weight of substrate.

Rate constants associated with both the overall substrate decomposition and the appearance of primary products were determined at low substrate conversions. Reaction orders were deduced by monitoring the dependence of pseudo-first-order rate constants on initial substrate concentration. For the vapor-phase pyrolyses, initial concentrations were directly proportional to initial substrate loading, whereas liquid-phase concentrations were varied through dilution with biphenyl.

Complete experimental details are available (Petrocelli, 1984).

Results

Experiments were directed toward determination of the identities and yields of the pyrolysis products, reaction

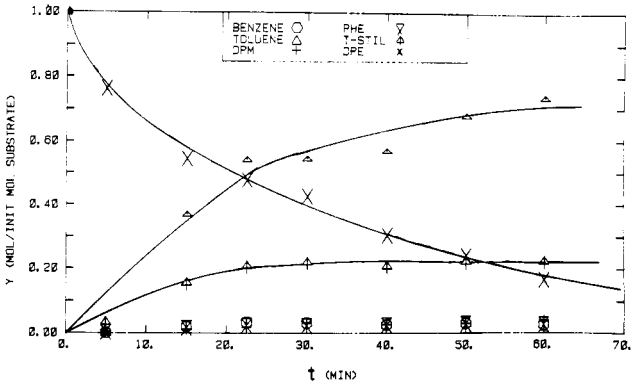

Figure 1. Diphenylethane pyrolysis products at 450 °C.

material balance closure, relationships among product proportions, likely reaction pathways, and pathway kinetics, including reaction order, rate constant, and Arrhenius parameters. Results are presented separately for each substrate.

Diphenylethane (DPE). DPE pyrolyses, studied at temperatures of 400, 450, and 550 °C and holding times of 900–10 800, 300–3600, and 90–600 s, respectively, were vapor phase except for certain experiments at 450 °C where liquid- and vapor-phase kinetics were compared. Average initial substrate concentration was 0.1 mol/L except for 450 °C, where reaction orders were determined by varying vapor-phase initial substrate concentrations from 0.04 to 1.37 mol/L.

DPE pyrolysis resulted in the formation of toluene and *trans*-stilbene, as major products, along with lesser amounts of benzene, ethylbenzene, styrene, diphenylmethane, *cis*-stilbene, and phenanthrene. The proportions of unidentified products were small, as indicated by material balance closures of 104.8 ± 4.7, 90.8 ± 7.5, and 99.4 ± 10.6% for pyrolysis at 400, 450, and 550 °C, respectively. Material balance uncertainties were computed as the square root of the sample variance, where the sample included all experiments with a given substrate at a given temperature. Two very minor peaks that appeared just prior to DPE and triphenylethylene on the OV-17 GC column were tentatively identified as 1,1-diphenylethane and 1,1,2-triphenylethane, respectively. Their proportions were always negligible.

Temporal variations of the pyrolysis products at 450 °C are presented in Figure 1, where product yields, in moles of product per initial moles of DPE, are plotted vs. pyrolysis holding time. These data show that while toluene and *trans*-stilbene were clearly predominant, these products and also benzene, diphenylmethane, and phenanthrene, having positive initial slopes in Figure 1, were primary reaction products. Experimental uncertainty associated with the low absolute yields of ethylbenzene and styrene prevented unequivocal designation of these as primary or secondary products.

Comparison of the proportions of the important products probes the likely operative reaction pathways. At DPE conversions of less than 8%, the ratio of twice the toluene yield to the stilbene yield was substantially unity. However, this ratio steadily increased with increasing DPE conversion, reaching a maximum of 6.7 at a conversion of 91%. This suggests that DPE pyrolysis reactions should include a primary pathway to toluene and stilbene products, with the latter capable of secondary decomposition.

Product relationships are developed further in Figure 2, a plot of the parameter R, defined as the ratio of the hydrogen consumed by the toluene and benzene formation pathways to the hydrogen evolved by the stilbene and

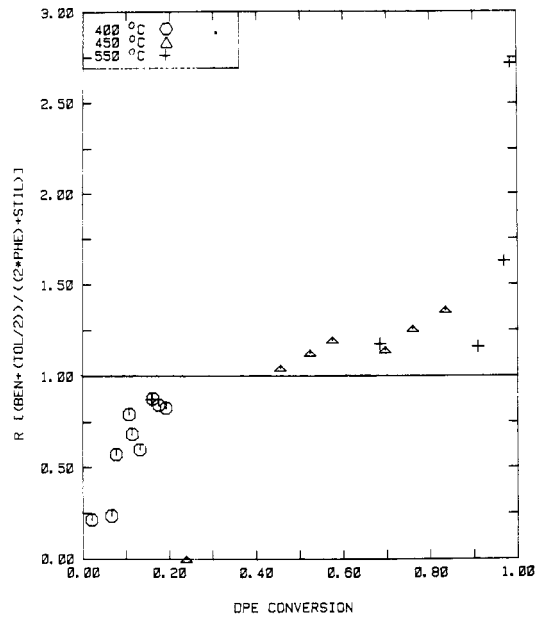

Figure 2. Ratio of H consumption to H evolution (R) from DPE pyrolysis.

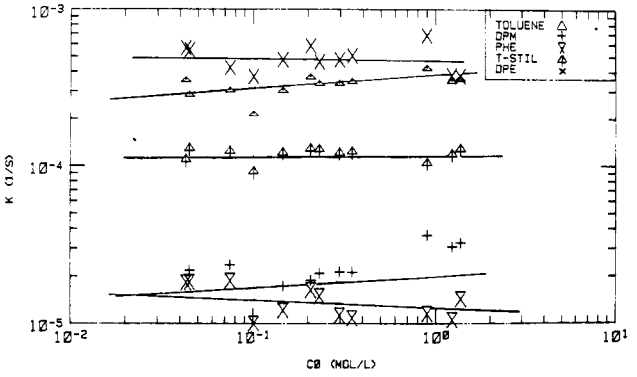

Figure 3. Dependence of DPE pyrolysis pseudo-first-order rate constants on initial substrate concentration.

phenanthrene formation pathways, vs. DPE conversion. Inspection of Figure 2 reveals that hydrogen formally evolved in stilbene and phenanthrene formation could account for the hydrogen consumed in the formation of toluene and benzene for DPE conversions of less than about 50%. However, R was significantly greater than unity at conversions in excess of 70%, which indicates that the formation of other unidentified, higher molecular weight, hydrogen-deficient (relative to DPE) species was concurrent with the formation of lighter hydrogen-rich products. Similarly, comparison of the sum of ethylbenzene plus styrene yields with benzene yields showed that essentially 1 mol of either ethylbenzene or styrene formed for each mole of benzene that appeared for DPE conversions of less than 40%. At higher DPE conversions, ethylbenzene plus styrene yield was consistently less than benzene yield, presumably due to secondary styrene decomposition to additional benzene, toluene, and ethylbenzene, among other products (Klein, 1981; Badger et al., 1958).

The foregoing suggested that a DPE pyrolysis reaction network should include primary pathways to toluene plus stilbene, benzene plus ethylbenzene or styrene, phenanthrene, and diphenylmethane products and also secondary decomposition of stilbene and styrene. The initial substrate concentration dependence of the pseudo-first-order rate constants associated with each primary pathway revealed reaction orders. These data are shown in Figure

Table II
Kraft Lignin Model Compound Pyrolysis Pathways and Kinetics

pathway			-log k^a								
reactant	product(s)	order	250 °C	300 °C	350 °C	400 °C	450 °C	550 °C	600 °C	log A^a	E^*, kcal/mol
diphenylethane	2 toluenes	1				4.66	3.28	1.92		10.2	45.3
	phenanthrene	1				5.96	4.70	3.03		10.1	49.2
	benzene	1				5.70	4.51	3.04		8.83	44.5
	stilbene	1				4.97	3.72	2.44		8.79	42.0
	diphenylmethane	1				5.64	4.87	3.17		8.00	42.2
cis-stilbene	*trans*-stilbene	1	4.65	3.39	2.38					9.47	33.8
stilbene	2 toluenes	2				4.43	3.81	2.50		6.19	32.9
	phenanthrene	1					6.07	3.92		11.6	58.6
	benzene	1					5.75	4.02		8.56	47.4
	diphenylethane	2				3.96	3.24			6.36	31.8
	diphenylmethane	1				5.19	4.94	3.86		2.22	23.1
diphenylmethane	benzene + toluene + fluorene	1						4.82	3.81	12.7	66.0
triphenylethylene	stilbene	1				5.96		4.16		3.92	30.4
	toluene + DPM	2				3.93		2.65		3.09	21.6

[a] k and A in s^{-1} or L mol^{-1} s^{-1}.

3 as a plot of $ln\ k$ (s^{-1}) vs. $ln\ C_0$ (mol/L) for overall substrate decomposition and primary product appearance pathways. Least-squares linear regression of $ln\ k$ vs. $ln\ C_0$, hereafter referred to as "least-squares analysis", revealed that each rate constant was independent of initial substrate concentration, and calculated reaction orders for overall DPE decomposition and toluene, stilbene, phenanthrene, and diphenylmethane appearance were 0.97 ± 0.05, 1.08 ± 0.04, 1.01 ± 0.03, 0.89 ± 0.05, and 1.07 ± 0.21. These were considered to be unity. The uncertainties associated with the calculated reaction orders were computed as the square root of the estimated variance of the slope of the linear regression of $ln\ k$ vs. $ln\ C_0$. Experimental uncertainty associated with the low benzene, ethylbenzene, and styrene yields prevented determination of their formation reaction orders. It is interesting that rate constants obtained for vapor- and mixed-phase pyrolyses at 450 °C were not significantly different.

Rate constants associated with each primary pathway are listed in Table II. Fitting these to the Arrhenius expression, $\log k = \log A - E^*/\theta$ with $\theta = 2.303RT$, revealed the Arrhenius parameters also listed. Arrhenius parameters for overall DPE decomposition were ($\log A$ (s^{-1}), E^* (kcal/mol)) = (10.5, 46.2).

***cis*- and *trans*-Stilbene.** Both *cis*-stilbene and *trans*-stilbene were pyrolyzed at temperatures of 250, 300, 350, 400, 450, and 550 °C for holding times ranging from 90 to 64 800 s. Reactor contents were in the liquid phase for pyrolyses at $T \leq 350$ °C and in the vapor phase for $T > 400$ °C. Pyrolysis at 400 °C resulted in an initial substrate distribution of 30% in the liquid phase and 70% in the vapor phase. The average initial substrate concentration for liquid-phase pyrolyses was 2.0 mol/L except for pyrolyses at 300 °C, where the cis–trans isomerization reaction order was investigated by varying initial concentrations from 0.2 to 2.0 mol/L through dilution with biphenyl. The initial substrate concentration for gas-phase pyrolyses was 0.1 mol/L except for pyrolyses at 450 °C, where *trans*-stilbene pyrolysis order was investigated by varying initial concentrations from 0.04 to 1.11 mol/L.

Cis–Trans Isomerization. Pyrolysis of either pure *cis*- or *trans*-stilbene at 250, 300, and 350 °C produced only a mixture of the two isomers as products, with *trans*-stilbene predominant in roughly 9/1 proportions. Material balance closures of 102.2 ± 3.4, 99.5 ± 5.0, and 98.1 ± 4.3%

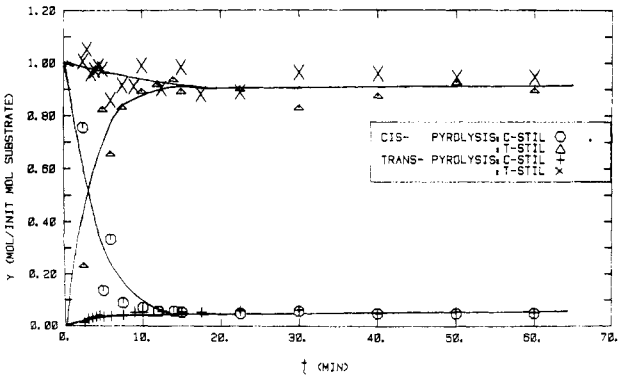

Figure 4. *cis*- and *trans*-stilbene isomerization reactions at 350 °C.

at 250, 300, and 350 °C, respectively, indicated that no other important products formed under these conditions. The temporal variations of *cis*- and *trans*-stilbene yields observed in pyrolysis of both at 350 °C are presented in Figure 4, which suggests that an equilibrium between the stilbenes was established from pyrolysis of either isomer. Calculated equilibrium constants K (mol of trans/mol of cis) of 29.2 and 17.1 at 300 and 350 °C, respectively, implied a heat of reaction of −7.6 kcal/mol for cis to trans isomerization.

Variation of initial *cis*-stilbene concentrations at 300 °C showed the cis–trans isomerization to be first order. Measurement of cis–trans isomerization rates from 250 to 350 °C yielded parameters shown in Table II; reverse reaction parameters, i.e., trans to cis isomerization, were less certain on account of the small product yields associated with the equilibrium limitations. The Arrhenius parameters for cis–trans isomerization show this reaction to be facile. Thus, not only was this the exclusive operative reaction pathway for *cis*-stilbene pyrolysis from 250 to 350 °C but also, as discussed below, cis–trans isomerization was overwhelmingly faster than any stilbene degradation pathway at $T \geq 400$ °C. This suggests that equilibration between isomers was fast relative to degradation reactions and that pyrolysis of either isomer was essentially equivalent to pyrolysis of a near-equilibrium mixture of the two isomers. This was verified experimentally, as degradative pyrolyses of *cis*- and *trans*-stilbene at $T \geq 400$ °C yielded virtually identical product spectra. Thus, the discussion

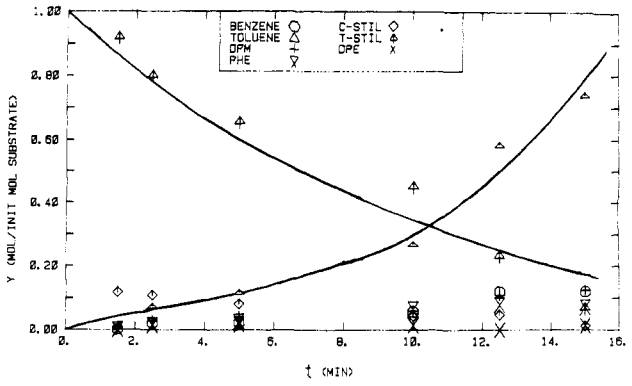

Figure 5. *trans*-Stilbene pyrolysis products at 550 °C.

to follow concerns *trans*-stilbene pyrolysis unless specific reference to *cis*-stilbene is made.

Stilbene Degradation. Stilbene decomposition yielded toluene, DPE, and diphenylmethane as major products along with lesser amounts of benzene, ethylbenzene, styrene, phenanthrene, and triphenylethylene. Yields of styrene, ethylbenzene, and triphenylethylene were uniformly small and difficult to quantify. Average material balance closures for stilbene pyrolyses were 94.7 ± 4.7, 91.2 ± 6.3, and 91.4 ± 10.9% at 400, 450, and 550 °C, respectively; material balance closure decreased with increasing pyrolysis temperature and substrate conversion. This information coupled with the detection of several small, unidentified GC peaks which eluted after all identified products to indicate that high molecular weight oligomers formed during stilbene pyrolysis.

The temporal variations of the yields of the important products from pyrolysis at 550 °C are shown in Figure 5. The positive initial slopes associated with each of DPE, benzene, diphenylmethane, toluene, and phenanthrene formation in Figure 5 indicate that these were primary pyrolysis products. It is noteworthy that DPE yield attains a maximum at about $t = 5$ min in Figure 5. Thus, it is likely that secondary DPE degradation contributed to the yields of benzene, toluene, and phenanthrene, even though these have been just noted to be primary pyrolysis products. Too, note that the yields of phenanthrene were always less than observed from pyrolysis of pure DPE at identical temperatures and times.

The foregoing suggested formulation of a stilbene pyrolysis reaction network to include primary pathways for isomerization and decomposition to each of DPE, benzene, diphenylmethane, toluene, and phenanthrene products. Pyrolyses at 450 °C and initial substrate concentrations of 0.04–1.11 mol/L revealed that overall *trans*-stilbene decomposition comprised a set of first- and second-order individual reactions. Overall stilbene conversion increased with increasing initial substrate concentration and least-squares analysis revealed an overall reaction order of 1.79 ± 0.25. Similar analyses revealed reaction orders of 1.00 ± 0.19, 1.06 ± 0.20, 1.73 ± 0.25, and 1.97 ± 0.20 for the formation of *cis*-stilbene, diphenylmethane, DPE, and toluene, respectively. Benzene and phenanthrene yields were too small to allow determination of their formation reaction orders, and these products were assumed to form via first-order pathways. The stilbene reaction network formulated thus included first-order pathways for stilbene isomerization and benzene, diphenylmethane, and phenanthrene appearance and second-order pathways for the formation of DPE and toluene.

Rate constants for each stilbene primary reaction pathway at 400, 450, and 550 °C are listed in Table II along with deduced Arrhenius parameters. It is notable that experiments at 450 °C spanned each of liquid-, vapor-, and mixed-phase pyrolysis and that kinetic results were demonstrably independent of the phase of the reactants.

Diphenylmethane (DPM). Vapor-phase DPM pyrolysis was examined at temperatures of 550 and 600 °C and holding times of 900–7200 and 120–1200 s, respectively. Average initial substrate concentrations were 0.1 mol/L except for a series of experiments at 550 °C where reaction orders were investigated by varying initial substrate concentrations from 0.14 to 0.75 mol/L.

Major product spectra components were benzene, toluene, and fluorene, along with smaller amounts of *cis*- and *trans*-stilbene, phenanthrene, and triphenylethylene. Total combined yields of the latter four products never exceeded 2%, by weight, of the initial substrate weight, which, however, was also the concentration of a *cis*-stilbene impurity in the unreacted DPM. Thus, only benzene, toluene, and fluorene were quantified in the analysis of DPM pyrolysis. Average material balance closures were 80.8 ± 10.9% at 550 °C and 84.6 ± 14.9% at 600 °C; material balance tended toward nonclosure as substrate conversion increased. A number of minor GC peaks were observed to elute at retention times greater than that of triphenylethylene, which suggests that high molecular weight oligomers formed during DPM pyrolysis.

The temporal variations of benzene, toluene, and fluorene yields at 550 °C showed that these were primary pyrolysis products. Product relationships are examined in Figure 6, parts A and B, the former plotting benzene yields vs. toluene yields and the latter plotting the sum of benzene and toluene yields vs. fluorene yield. Entries in Figure 6A, falling closely about the line $y_{BEN} = y_{TOL}$, show that benzene and toluene were produced in essentially stoichiometric proportions. Figure 6B shows that the sum of benzene and toluene yields generally exceeded twice the fluorene yield, indicating that not only fluorene appearance but also oligomer formation supplied the necessary hydrogen for the benzene and toluene products.

The foregoing suggested formulation of a primary DPM pyrolysis pathway to account for the formation of stoichiometric proportions of benzene and toluene and also fluorene and other hydrogen-poor species. The dependence of pseudo-first-order rate constants on initial substrate concentrations revealed apparent reaction orders of 0.7 ± 0.3, 1.2 ± 0.1, 1.3 ± 0.2, and 1.2 ± 0.3 on the basis of overall DPM decomposition and benzene, toluene, and fluorene appearance, respectively. The DPM pyrolysis pathway was thus considered to be first order, for which rate constants and Arrhenius parameters are listed in Table II.

Triphenylethylene (TPE). Triphenylethylene (TPE) was pyrolyzed at 400 and 550 °C for holding times of 600–10 800 and 60–900 s, respectively. Pyrolyses at 400 °C were liquid phase with average initial substrate concentrations of 1.1 mol/L. The gas-phase pyrolyses at 550 °C were with initial substrate concentrations of 0.1 mol/L except where reaction orders were investigated by varying initial concentrations from 0.06 to 0.56 mol/L.

TPE pyrolysis products included benzene, toluene, DPM, DPE, fluorene, stilbene, and phenanthrene. Average material balance closures were 92.8 ± 4.8% at 400 °C and 80.6 ± 9.0% at 550 °C. In general, but especially at 550 °C, material balance nonclosure was attended by detection of several high molecular weight products that could not be identified. TPE was relatively unreactive at 400 °C as the DPM and toluene major products were accompanied by small amounts of other products; no fluorene was observed at 400 °C, and phenanthrene was detected only

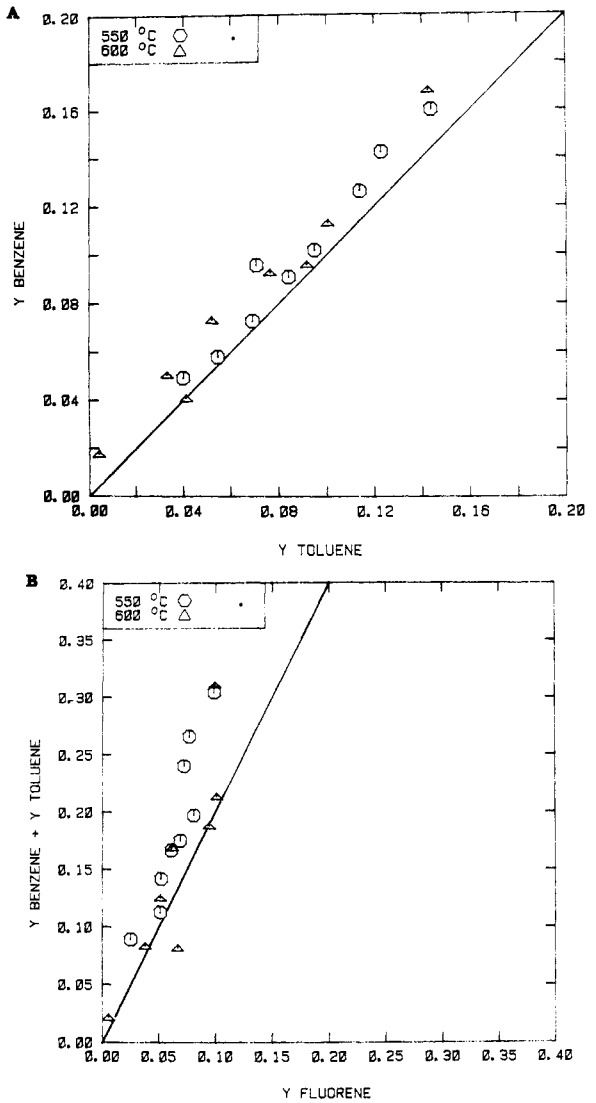

Figure 6. (A) Benzene vs. toluene yields from diphenylmethane pyrolysis. (B) (Benzene + toluene) vs. fluorene yields from diphenylmethane pyrolysis.

after a 20-min holding time. Reactivity was more appreciable at 550 °C, where the most primary experimental data were obtained at TPE conversions of 17%. This prevented unequivocal discrimination between primary and secondary products, but the presence of DPM, toluene, benzene, and stilbene from pyrolysis at 400 °C, however, suggests that these products were most likely primary.

Comparison among the product yields at 550 °C showed that equimolar proportions of toluene and DPM were produced and also that yields of benzene were comparable to the sum of DPE and stilbene yields. This information and also the negligible yields of either fluorene or phenanthrene at 400 °C and TPE conversions of up to 20% suggested that the TPE pyrolysis reaction network should contain primary routes to toluene plus DPM and benzene plus stilbene or DPE; secondary pathways would contribute to fluorene and phenanthrene yields. Since the yields of these fused-ring products were too large to be accounted for solely by secondary decomposition of DPM (to fluorene) and stilbene (to phenanthrene), it is likely that unobserved phenyl-substituted fluorene and phenanthrene species were also present during pyrolysis and served as fluorene and phenanthrene precursors.

Experiments at 550 °C spanning initial substrate concentrations from 0.06 to 0.56 mol/L revealed that apparent first-order rate constants associated with benzene (calculated reaction order = 1.04 ± 0.14), DPE, stilbene, fluorene, and phenanthrene yields were all independent of initial TPE concentration. The calculated reaction order for both toluene and DPM appearance of 1.84 ± 0.15 was interpreted as second order, and overall TPE decomposition occurred with apparent 1.74 ± 0.12 order kinetics at the conditions studied. Rate constants and estimated Arrhenius parameters for both TPE primary pyrolysis pathways are listed in Table II.

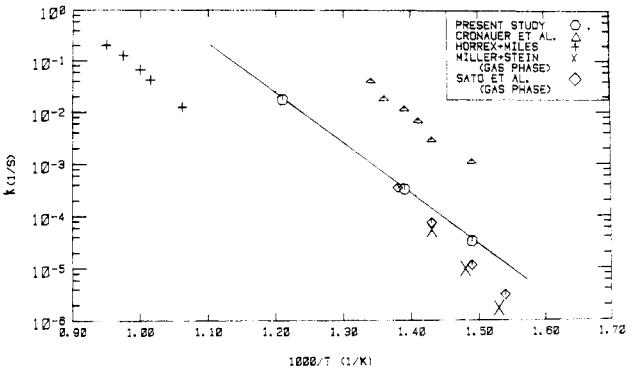

Figure 7. DPE pyrolysis Arrhenius diagram.

Discussion

We here consider the present results in light of both previous experimental model compound and Kraft lignin pyrolyses.

Model Compound Reaction Pathways. The present DPE pyrolysis product spectra, containing the primary products toluene, benzene, stilbene, phenanthrene, and DPM and also the products ethylbenzene, styrene, and higher molecular weight oligomers are in accord with those previously reported. Comparison with the neat pyrolysis information of Vernon (1980), Sweeting and Wilshire (1962), and Benjamin (1978) is most favorable; greater proportions of toluene were observed elsewhere (Collins et al., 1977; Benjamin et al., 1978; Kamiya, 1979; Cronauer et al., 1978) from pyrolysis in hydrogen-donor solvents.

The temperature dependence of the observed DPE decomposition rate constants corresponds to first-order Arrhenius parameters (log A, E^*) = (10.5, 46.2). These compare with values deduced by Horrex and Miles (1951) of (9.3, 48.0), Cronauer et al. (1978) of (10.8, 48.1), Sato et al. (1978) of (liquid phase: 14.4, 61.5; gas phase: 14.8, 60.4), and Miller and Stein (1979) of (liquid phase: 16.0, 61; gas phase: 14.9, 61). This information is summarized in Figure 7, an Arrhenius diagram of the rate constants from which these differing Arrhenius parameters were calculated. Individual rate constants determined here are seen to fall within the range of previously reported values. However, an obviously unequivocal set of Arrhenius parameters remains unclear. This renders mechanistic interpretation of the Arrhenius parameters difficult; too, the coincidence of neat and solvent-diluted rate constants is consistent with either a free radical mechanism with a first-order solvent-independent rate-determining step or Virk's (1979) concerted pericyclic mechanism as operative during pyrolysis.

Stilbene pyrolysis comprised a facile, low-temperature isomerization reaction and also higher temperature fragmentation pathways. Deduced isomerization equilibrium constants of 29.2 and 17.1 at 300 and 350 °C, respectively, compare with previously reported values of 14.63 and 11.99 at 320 and 341 °C, respectively (Kistiakowsky and Smith, 1934). Implied reaction enthalpies of −7.6 and −3.0 kcal/mol, the latter deduced by Kistiakowsky and Smith assuming zero entropy change of isomerization, also com-

pare reasonable well. Stilbene isomerization rate constants found here, by Kistiakowsky and Smith (1934), and by Taylor and Murray (1938) at 300 °C were respectively 4.10 × 10^{-4}, 2.98 × 10^{-4}, and 2.52 × 10^{-4} s^{-1}; Arrhenius parameters were respectively (log A, E^*) = (9.47, 33.8), (12.8, 42.8), and (10.4, 36.7).

When stilbene decomposition did occur, pyrolysis of either pure isomer was equivalent to pyrolysis of a virtual equilibrium mixture of the two. Decomposition products, mainly toluene, DPE, and DPM, along with lesser amounts of benzene, ethylbenzene, styrene, phenanthrene, and triphenylethylene were like those found by Benjamin (1978).

As regards stilbene pyrolysis mechanisms, the second-order pathway to DPE is consistent with a disproportionation that would be attended by formation of a diphenylacetylene intermediate. It is curious that yields of phenanthrene were always higher from DPE than stilbene pyrolysis at identical conditions. Thus stilbene was not a unique phenanthrene precursor, and, hence, this reaction path did not proceed solely through the apparently obvious dehydrogenative fusion of *cis*-stilbene.

Important identified DPM pyrolysis products were benzene, toluene, and fluorene. Hydrogen formally evolved in the formation of fluorene was less than the hydrogen consumed in the near-equimolar formation of benzene and toluene. This is consistent with the Sweeting and Wilshire (1962) report of benzene, toluene, fluorene, and DPM yields of 0.54, 0.54, 0.92, and 93.3 wt %, respectively, for DPM pyrolysis at 700 °C, which showed that formal hydrogen liberation during fluorene formation failed to account for hydrogen consumption in the near-equimolar formation of benzene and toluene; these investigators' material balance closure was also less than 100%. Madison and Roberts (1958) also found heavy residual products from DPM pyrolysis.

Present and previous results are consistent with an operative pyrolysis mechanism comprising a highly energetic free-radical scission of DPM to phenyl and benzyl radicals, followed by hydrogen abstraction reactions which generate benzene, toluene, fluorene, and other unidentified heavy products.

Important TPE pyrolysis products were benzene, toluene, DPM, DPE, fluorene, stilbene, and phenanthrene, and material balance nonclosure at high substrate conversions coincided with the formation of several higher molecular weight products that were not identified. Collins et al. (1977) found DPM and toluene as the only significant pyrolysis products at 380 °C and 1.5 h in tetralin.

Two reaction pathways were observed at 550 °C. The first was first-order decomposition to benzene and stilbenzene and likely involved free-radical fission reactions. The second pathway, second order in TPE concentration, led to DPM and toluene products and likely proceeded via a free-radical chain pathway or a simple disproportionation route akin to the stilbene pathway to DPE noted earlier.

It is interesting to view TPE pyrolysis as a superposition of the reactions of the DPM and stilbene moieties TPE comprises. This is illustrated in Figure 8, where formation of benzene and stilbene from TPE is formally similar to the formation of benzene and toluene from DPM. Both of these reactions were observed to be first order with rate constants $k_{550°C}$ = 6.9 × 10^{-5} and 1.8 × 10^{-5}, respectively. Formation of toluene and DPM from TPE, then, is formally similar to the formation of two toluene molecules from stilbene. Both reactions were observed to be second order with rate constants $k_{550°C}$ = 2.2 × 10^{-3} and 3.14 × 10^{-3} L/(mol·s), respectively, at the conditions studied.

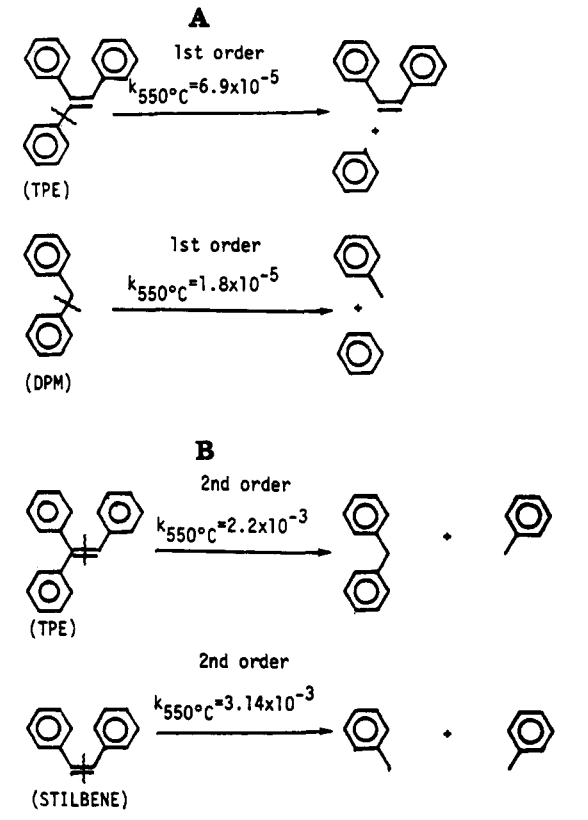

Figure 8. Triphenylethylene (TPE) pyrolysis as a superposition of diphenylmethane (DPM) and stilbene pyrolysis reactions: (A) TPE and DPM reaction path analogies; (B) TPE and stilbene reaction path analogies.

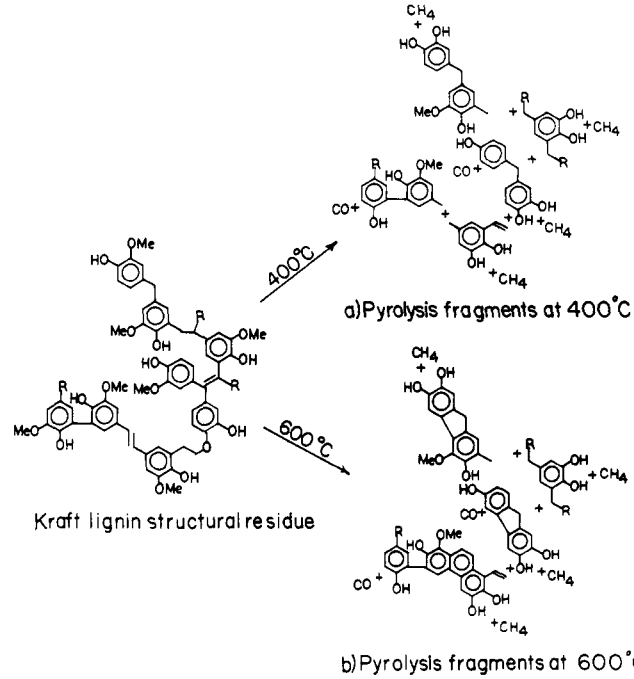

Figure 9. Application of model compound reaction pathways to Kraft lignin pyrolysis.

These analogies also suggest that products like 1,1,2-triphenylethane and 9-phenylphenanthrene also formed during TPE pyrolysis, since DPE and phenanthrene were stilbene pyrolysis products.

Implications to Kraft Lignin Pyrolysis. The present results combine to suggest that Kraft lignin pyrolysis contains the reactions illustrated in Figure 9. During pyrolysis at temperatures of, say, 400–500 °C, DPE, stil-

bene, and phenethyl phenyl ether (Klein and Virk, 1983) linkages will be reactive, while DPM, biphenyl, and diphenyl ether (Klein, 1981) links will be rather unreactive. This implies that roughly half of a Kraft lignin's interunit links will cleave, as illustrated in Figure 9a, yielding single-ring phenolic products and a residual lignin and multiring phenolic fragments that contain mainly DPM, biphenyl, and diphenyl ether bonds. Pyrolysis at higher temperatures, say, 500–600 °C, is shown as Figure 9b and should generate additional single-ring phenolics through cleavage of the more thermally stable DPM bonds and also yield dervatives of fluorene, phenanthrene, and other fused-ring products through condensation reactions quite like those observed here in DPM, DPE, and stilbene pyrolysis. It is rather surprising, however, that the fluorene, naphthalene, and anthracene products observed from Kraft lignin microwave pyrolysis (Chan and Krieger, 1981) were not hydroxy substituted.

The significance of Kraft lignin stilbene and DPE moieties is illustrated through comparison among Kraft lignin, stilbene, and DPE pyrolyses. In tetralin, stilbene saturates readily to DPE (Benjamin, 1978), which in turn fragments to toluene with high selectivity. Thus, since neat stilbene and DPE pyrolyses yield not only toluene but also significant quantities of hydrogen-poor higher molecular weight products, yields of single-ring phenols from pyrolysis of Kraft lignin in tetralin should be, and have been observed to be, higher than from neat pyrolysis (Jegers, 1982).

The present reaction pathway and kinetics results can be used in simulation of Kraft lignin pyrolysis (Petrocelli, 1983); this work is to be described more fully in a subsequent report. In brief, a statistical interpretation of lignin allows these model compound reaction pathways to be superimposed on chemically similar lignin moieties. Although the model compounds examined here are devoid of the oxygen-containing substituents found on their lignin analogues, it is reasonable to expect the oxygenated substituents to influence significantly only the reaction rate and not the formal reaction pathway. For example, whereas the present and also previous (Madison and Roberts, 1958; Sweeting and Wilshire, 1962) pyrolyses of diphenylmethane showed benzene and toluene to be the important light products, phenol and toluene were the predominant light products from the faster pyrolysis of (*o*-hydroxyphenyl)phenylmethane (Benjamin et al., 1978; Klein, 1981). Likewise, the reactants in the pairs cinnamic acid/ferulic acid (Klein, 1981; Jungten and van Heek, 1968) and benzaldehyde/vanillin (Brower, 1977; Klein, 1981) undergo analogous reaction pathways that are more rapid for the hydroxyl-substituted substrates. The lignin pyrolysis simulation model can account for this kinetic effect easily.

In light of the present experimental results, then, predicted products include primarily methyl-substituted single-ring phenols, which follow from the prevalence of toluene from DPE, DPM, and stilbene pyrolyses. Similarly, lesser experimental yields of benzene, styrene, and ethylbenzene products from these substrates correspond to model predictions of lesser yields of hydride-, vinyl-, and ethyl-substituted phenols, respectively. Experimental condensation pathways leading to phenanthrene and fluorene allow simulation prediction of hydroxyl-substituted phenanthrene and fluorene derivatives. Quantitative comparison of simulation predictions with actual lignin pyrolyses is encouraging (Petrocelli and Klein, 1982).

Conclusions

Important conclusions arising from the present analyses and experimental results are as follows:

(1) Kraft pulping processes render the residual lignin a single-ring phenolic copolymer whose aromatic units are connected by relatively few types of interunit linkages. Important among these are linkages that can be mimicked by diphenylethane, stilbene, diphenylmethane, and triphenylethylene model compounds.

(2) Toluene was the major product obtained from pyrolysis of diphenylethane and stilbene and a major coproduct obtained from pyrolysis of diphenylmethane and triphenylethylene. This suggests that single-ring phenols formed from lignin pyrolysis should be predominantly methyl substituted.

(3) Reaction pathways to fused-ring products, namely, phenanthrene from stilbene and diphenylethane pyrolyses and fluorene from diphenylmethane pyrolysis, were observed and quantified. These are noteworthy because mechanisms for formation of these and similar fused-ring products during actual lignin thermolyses have not been set forth previously. Phenanthrene yields were always higher from diphenylethane pyrolysis than from stilbene pyrolysis, which suggests its formation is not exclusively through a *cis*-stilbene intermediate.

(4) Isomerization of either *cis*- or *trans*-stilbene to an equilibrium mixture of the two was rapid at temperatures near 250 °C, whereas decomposition reactions were appreciable only at 400 °C; trans was always the predominant isomer in the equilibrium mixture. This suggests that nominal pyrolysis of either isomer alone was actually equivalent to decomposition of a near-equilibrium mixture of the two.

Acknowledgment. We acknowledge the financial support of the University of Delaware Research Foundation.

Registry No. Kraft lignin, 8068-05-1; *trans*-stilbene, 103-30-0; 1,2-diphenylethane, 103-29-7; *cis*-stilbene, 645-49-8; diphenylmethane, 101-81-5; triphenylethylene, 58-72-0.

References and Notes

(1) Badger, G. M.; Buttery, R. G. *J. Chem. Soc.* **1958**, *2*, 2458.
(2) Benjamin, B. M. *Fuel* **1978**, *57*, 378.
(3) Benjamin, B. M.; Raaen, V. F.; Maupin, P. H.; Brown, L. L.; Collins, C. J. *Fuel* **1978**, *57*, 69.
(4) Brower, K. R. *Fuel* **1977**, *56*, 245.
(5) Chan, R. W.; Krieger, B. B. *J. Appl. Polym. Sci.* **1981**, *26*, 1.
(6) Collins, C. J.; Raaen, V. F.; Benjamin, B. M.; Kabalka, G. W. *Fuel* **1977**, *56*, 107.
(7) Connors, W. J.; Johanson, L. N.; Sarkanen, K. V.; Winslow, P. *Holzforschung* **1980**, *34*, 29.
(8) Cronauer, D. C.; Jewell, D. M.; Shah, Y. T.; Kueser, K. A. *Ind. Eng. Chem. Fundam.* **1978**, *17*, 291.
(9) Freudenberg, K.; Neish, A. C. "Constitution and Biosynthesis of Lignin"; Springer-Verlag: New York; 1968.
(10) Glasser, W. G.; Glasser, H. R.; Morohoshi, N. *Macromolecules* **1981**, *14*, 253.
(11) Graef, M.; Allan, G. G.; Krieger, B. B. *Prepr., Div. Pet. Chem., Am. Chem. Soc.* **1979**, *24*, 432.
(12) Horrex, C.; Miles, S. E. *Discuss. Faraday Soc.* **1951**, *10*, 187.
(13) Iatridis, B.; Gavalas, G. R. *Ind. Eng. Chem. Prod. Res. Dev.* **1979**, *18*, 127.
(14) Jegers, E. H. M.Ch.E. Thesis, University of Delaware, Newark, DE, 1982.
(15) Juntgen, H.; van Heek, K. H. *Fuel* **1968**, *47*, 103.
(16) Kamiya, Y.; Yao, T.; Oikawa, S. *Prepr. Pap.–Am. Chem. Soc., Div. Fuel Chem.)* **1979**, *24*, 116.
(17) Kistiakowsky, G. B.; Smith, W. R. *J. Am. Chem. Soc.* **1934**, *56*, 638.
(18) Klein, M. T. Sc.D. Thesis, M.I.T., Cambridge, MA, Feb 1981.
(19) Klein, M. T.; Virk, P. S. *Ind. Eng. Chem. Fundam.* **1983**, *22*, 35.
(20) Klein, M. T.; Virk, P. S. MIT *Press Energy Lab Ser.* **1981**, *5*.
(21) Madison, J. J.; Roberts, R. M. *Ind. Eng. Chem.* **1958**, *50*, 237.
(22) Marton, J. In "Lignin"; Sarkanen, Ludwig, Eds.; Wiley: New York, 1971.

(23) Miller, R. E.; Stein, S. E. *Prepr. Pap.-Am. Chem. Soc., Div. Fuel Chem.* **1979**, *24*, 271.
(24) Panvelker, S. V.; Shah, Y. T.; Cronauer, D. C. *Ind. Eng. Chem. Fundam.* **1982**, *21*, 236.
(25) Petrocelli, F. P. M.Ch.E. Thesis, University of Delaware, in preparation.
(26) Petrocelli, F. P.; Klein, M. T. "Simulation of Kraft Lignin Pyrolysis"; Proceedings, Fundamentals of Thermochemical Biomass Conversion: An International Conference, Estes Park, CO, 1982 (accepted).
(27) Poutsma, M. L. *Fuel* **1980**, *59*, 335.
(28) Sato, Y.; Yamakawa, T.; Onishi, R.; Kameyama, H.; Amano, A. *J. Jpn. Pet. Inst.* **1978**, *21*, 114.
(29) Sweeting, J. W.; Wilshire, J. F. K. *Aust. J. Chem.* **1962**, *15*, 89.
(30) Taylor, T. W. T.; Murray, A. R. *J. Chem. Soc.* **1938**, 2078.
(31) Vernon, L. W. *Fuel* **1980**, *59*, 102.
(32) Virk, P. S. *Fuel* **1979**, *58*, 149.
(33) Woodward, R. B.; Hoffmann, R. "The Conservation of Orbital Symmetry"; Verlag Chemie: Weinheim, 1970.

Molecular Modeling of Polymer–Dye Complexes Involving Homopolymers of Poly(*N*-vinylimidazole) and Methyl Orange

B. J. Orchard

Department of Macromolecular Science, Case Western Reserve University, Cleveland, Ohio 44106

J. S. Tan

Research Laboratories, Eastman Kodak Company, Rochester, New York 14650

A. J. Hopfinger*

Department of Macromolecular Science, Case Western Reserve University, Cleveland, Ohio 44106. *Received March 14, 1983*

ABSTRACT: Molecular modeling was used to study the intramolecular conformational behavior of neutral and fully quaternized poly(*N*-vinylimidazole) and the anionic form of methyl orange. Subsequently, intermolecular modeling of polymer–dye interactions was performed on the basis of the intramolecular findings. The purpose of the intermolecular studies was to identify a molecular geometry of the polymer–dye complex whose thermodynamic properties are consistent with experimental observations. This was achieved by assuming an isotactic chain segment of the polymer in a 3/1 helical conformation and an effective dielectric constant (in the Coulomb atom-pair potential) of 30. The polymer–dye binding complex is characterized by partial insertion (intercalation) of a phenyl ring of the dye between spatially adjacent polymer side-chain rings with the sulfonate of the dye located as close as possible to the charged imidazole nitrogen of the polymer.

Introduction

Tan and Handel[1] have investigated the binding behavior of methyl orange to homopolymers and copolymers of quaternized poly(*N*-vinylimidazoles) (PVI) in the presence of various counterions. The principal findings from these studies are as follows: (1) The apparent polymer–dye binding constant, log K_{app}, increases as the extent of binding, r, increases. (2) K_{app} for a given r and added salt decreases with an increase in ionic strength. The stoichiometry of the site–dye complex approaches unity as the polymer solution is saturated with excess dye. Stoichiometric unity is not realized for uncharged polymers. (3) The binding strength (or $-G$) at a given r decreases in the following order: BPVI (benzyl chloride quaternized PVI) > MPVI (methyl bromide quaternized PVI) > PVI. (4) The dye binding to MPVI and BPVI is identical in MeOH and is much weaker than in aqueous media. (5) The enthalpy of binding ($\Delta H°$) is exothermic and independent of ionic strength and/or type of counterion present in solution. (6) The $-\Delta H°$ of binding at low saturation (r = 0.01) decreases in the following order: BPVI > PVI > MPVI.

Some conclusions and an interpretation of the binding behavior can be summarized as follows: (1) Electrostatic and steric (van der Waals) interactions act jointly in controlling polymer–dye binding. The stoichiometry of the polymer–dye complex is governed by electrostatics (charge). (2) There is a direct competition between the dye and the counterions for polymer binding sites. (3) The electrostatic interactions have a net effect on the entropic contribution to binding and a lesser extent on the enthalpy. The measured $-\Delta H°$ of binding arises from polymer–dye (electrostatic and van der Waals) and dye–dye interactions (van der Waals). (4) An effective molecular "dielectric constant" of ~30 can be used to explain the observed thermodynamic properties when charge–charge interactions are modeled by a simple Coulombic function. (5) There is cooperative bound dye–dye interaction as opposed to independent-site binding. The degree of cooperativity decreases as the binding approaches saturation.

The goal of the work reported here has been to identify intermolecular charged polymer–dye molecular structures that are energetically stable and consistent with the observations and conclusions described above. A necessary corollary to this work has been an analysis of the molecular energetics, especially factors affecting electrostatic interactions. Molecular modeling has been carried out within the fixed-valence geometry molecular-mechanics formalism[2] for charged polymer segments and/or the dyes. The CHEMLAB molecular modeling laboratory[3] was used to perform the computational chemistry.

An important consideration, and likely limitation, of the results reported in this paper involves polymer tacticity. The experimental studies have used atactic polymer samples. It is not possible to explicitly model atactic structures in conformational structure calculations, owing to the random stereochemical behavior. We have considered only chain segments of all-isotactic and all-syndiotactic struc-

* Alternative address: Department of Medicinal Chemistry, Searle Research and Development, 4901 Searle Parkway, Skokie, IL 60077.

0024-9297/84/2217-0169$01.50/0